Figure S1

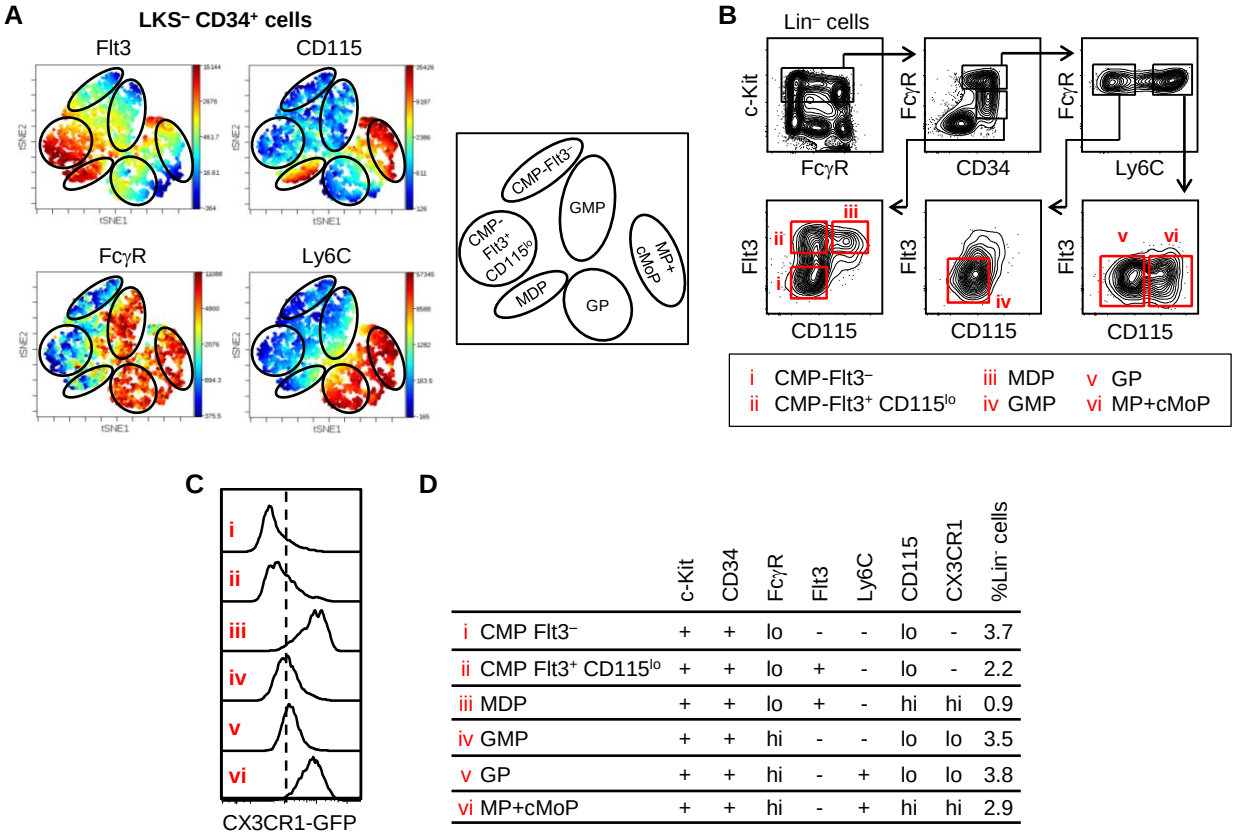

	c-Kit	CD34	FcγR	Flt3	Ly6C	CD115	CX3CR1	%Lin⁻ cells
i CMP Flt3⁻	+	+	lo	-	-	lo	-	3.7
ii CMP Flt3⁺ CD115lo	+	+	lo	+	-	lo	-	2.2
iii MDP	+	+	lo	+	-	hi	hi	0.9
iv GMP	+	+	hi	-	-	lo	lo	3.5
v GP	+	+	hi	-	+	lo	lo	3.8
vi MP+cMoP	+	+	hi	-	+	hi	hi	2.9

Figure S1. Characterization of myeloid progenitors from mouse bone marrow. (related to Figure 1) (A) MACS-sorted lineage-negative (Lin⁻) mouse bone marrow cells were evaluated by flow cytometry (c-Kit [CD117], Sca-1, CD34, FcγR [CD16 and CD32], Ly6C, Flt3, CD115). c-Kit⁺ Sca-1⁻ CD34⁺ cells were gated and viSNE analysis was performed using Cytobank. Flt3, CD115, FcγR and Ly6C expression was visualized in a stacked dot plot of tSNE1 and tSNE2 (left panels) to facilitate identification of progenitor populations (right panel). (B) Flow cytometry gating of bone marrow Lin⁻ cells for progenitor identification and sorting. Clear separation of the FcγR^{lo} and FcγR^{hi} gates is very important for optimal separation of the progenitor fractions. (C) CX3CR1 expression by progenitor subsets from CX3CR1-GFP reporter mice was assessed by flow cytometry. (D) Summary of surface marker expression by myeloid progenitor subsets.

Figure S2

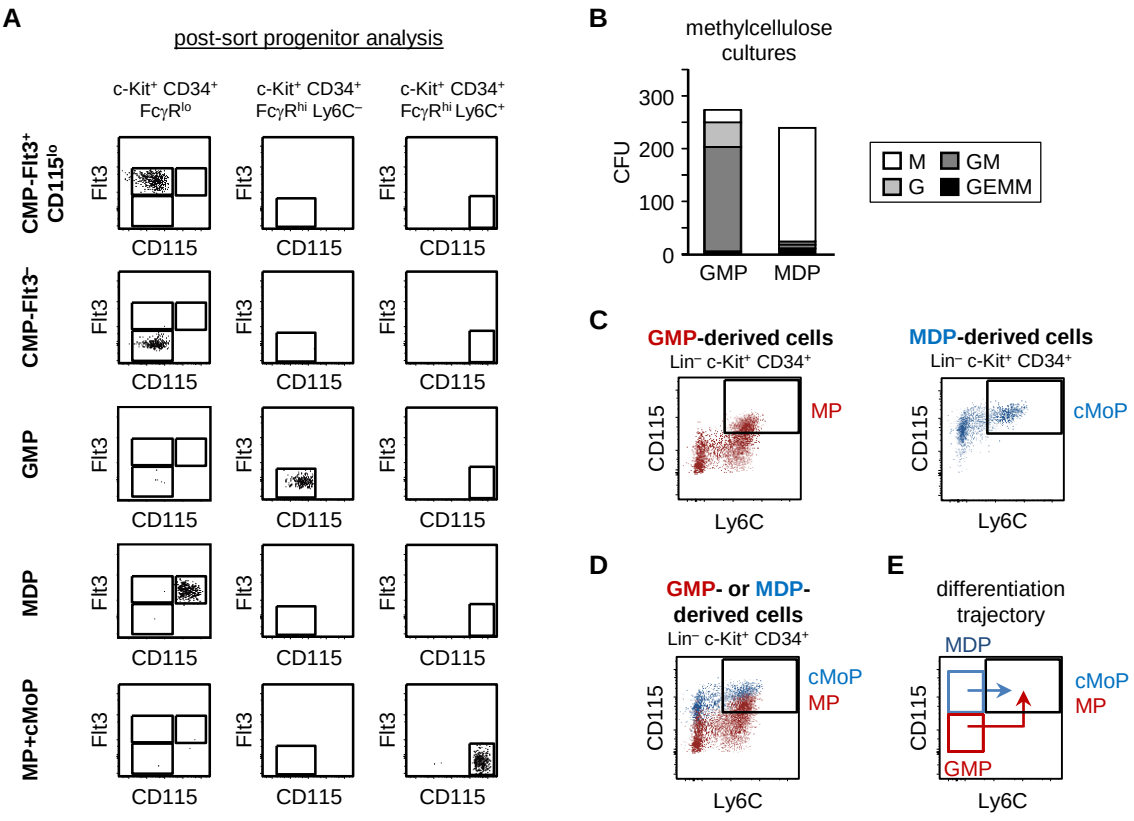

Figure S2. Characterization of myeloid progenitors from mouse bone marrow. (related to Figure 1) (A) Post-sort analysis of progenitor subsets after FACS sorting from mouse bone marrow. (B) 1000 GMPs or MDPs were seeded in methylcellulose medium, and colonies were evaluated 1 week later (M – monocyte, G – granulocyte, GM – granulocyte-monocyte, GEMM – granulocyte-erythrocyte-megakaryocyte-monocyte). (C-D) GMPs and MDPs were cultured *in vitro* with M-CSF for 48 hours, and MP or cMoP production was assessed by flow cytometry (overlaid in D). (E) Trajectory of monocyte-committed progenitor (MP or cMoP) production by GMPs and MDPs.

Figure S3

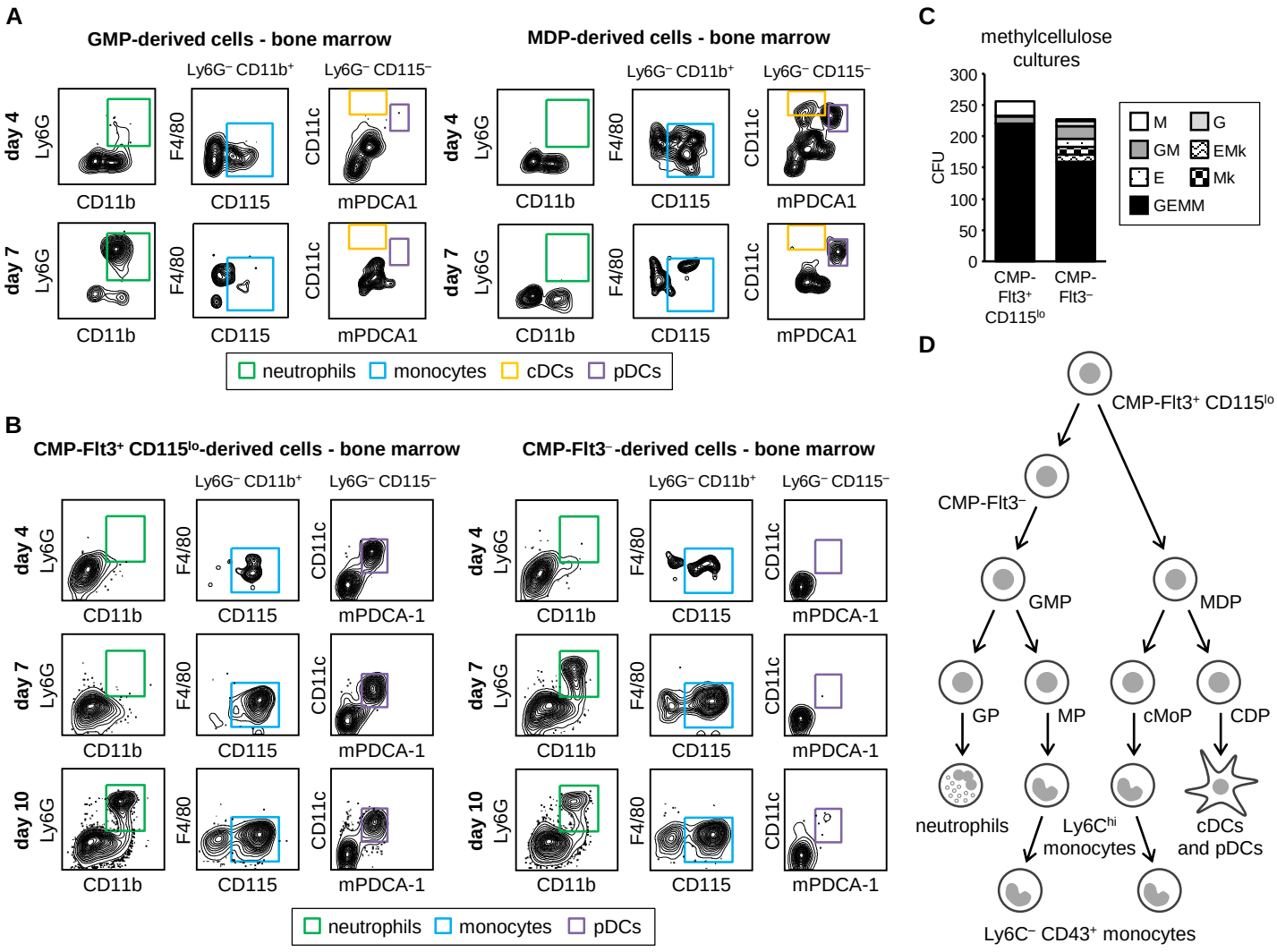

Figure S3. Myeloid cell production by CMP subsets. (related to Figure 1)

(A-B) The progeny of adoptively transferred GMPs and MDPs (A) and CMP-Flt3$^+$ CD115^{lo} and CMP-Flt3$^-$ cells (B) from donor (CD45.2) mice were identified by flow cytometry of recipient (CD45.1) bone marrow cells on the days indicated. (C) 1000 CMP-Flt3$^+$ CD115^{lo} and CMP-Flt3$^-$ cells per well were plated in methylcellulose media and colonies were counted after 1 week of culture. G – granulocyte, M – monocyte, E – erythrocyte, Mk – megakaryocyte, GM – granulocyte + monocyte, EMk – erythrocyte + megakaryocyte, GEMM – granulocyte + erythrocyte + monocyte + megakaryocyte. (D) Model of neutrophil, monocyte and DC production by CMP-Flt3$^+$ CD115^{lo} cells, with 2 independent pathways of monocyte differentiation via i) CMP-Flt3$^-$ cells, GMPs and MPs, and ii) MDPs and cMoPs.

Figure S4

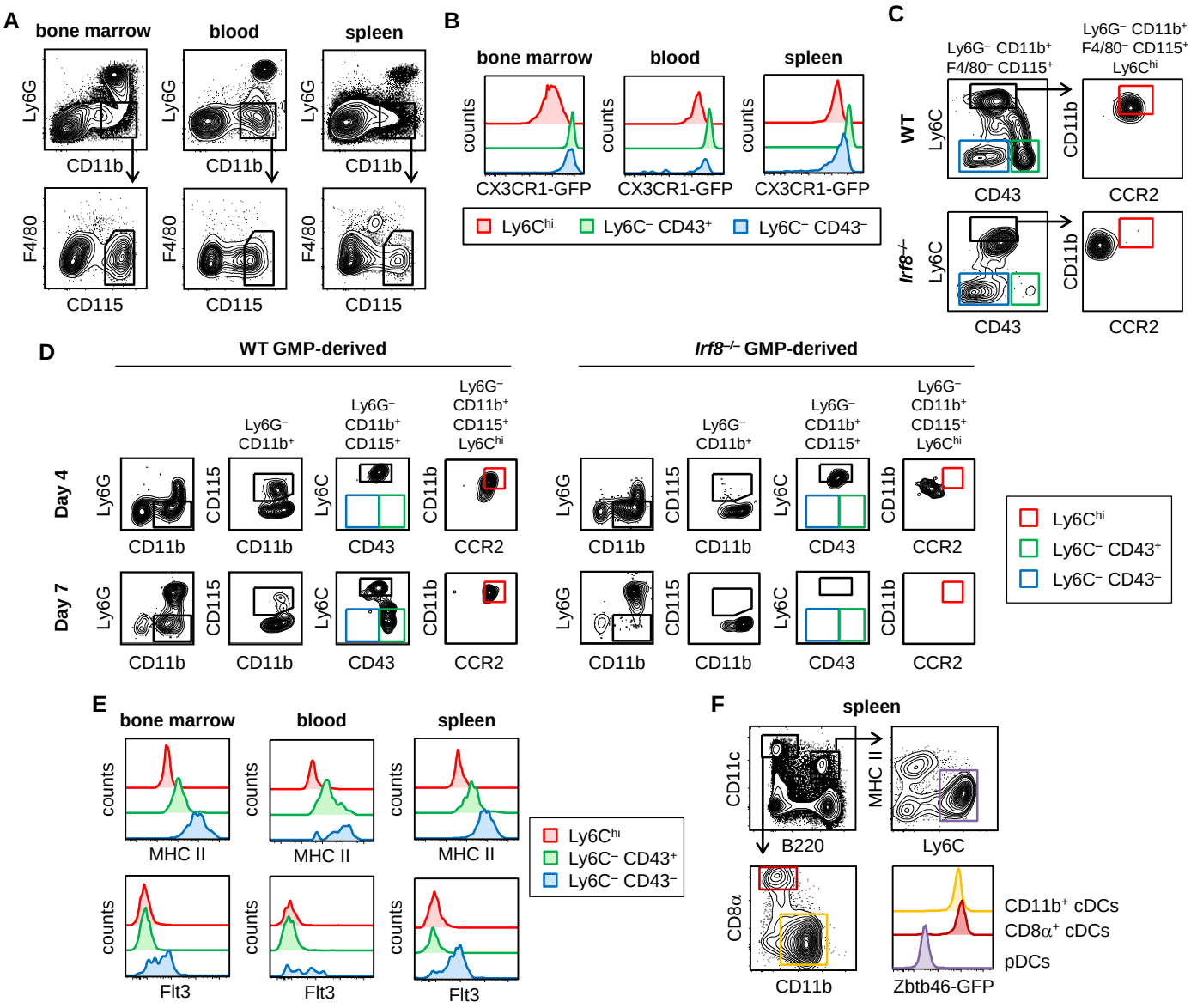

Figure S4. Profiling of GMP- and MDP-derived monocyte subsets. (related to Figure 2)

(A) Flow cytometry gating strategy for characterization of CD11b$^+$ CD115$^+$ cells in the bone marrow, blood and spleen. (B) CD11b$^+$ CD115$^+$ cells from the bone marrow, blood and spleen of CX3CR1-GFP reporter mice were analyzed by flow cytometry to assess CX3CR1 expression by the Ly6C^{hi}, Ly6C$^–$ CD43$^+$ and Ly6C$^–$ CD43$^–$ subsets. (C) For assessment of fully differentiated Ly6C^{hi} monocytes in *Irf8*-deficient (plus WT and *Nur77 (Nr4a1)*-deficient) mice, monocytes were also gated on CCR2$^+$ cells. (D) Flow cytometry gating strategy for assessing production of the Ly6C^{hi} (and CCR2$^+$), Ly6C$^–$ CD43$^+$ and Ly6C$^–$ CD43$^–$ subsets of CD11b$^+$ CD115$^+$ cells by adoptively transferred GMPs, MDPs and MPs+cMoPs from CD45.2 donor mice. Gating of GMP-derived cells is shown. (E) MHC II and Flt3 expression by the Ly6C^{hi}, Ly6C$^–$ CD43$^+$ and Ly6C$^–$ CD43$^–$ subsets of CD11b$^+$ CD115$^+$ cells from the bone marrow, blood and spleen was assessed by flow cytometry. (F) Expression of Zbtb46 by splenic cDCs and pDCs from Zbtb46-GFP reporter mice was assessed by flow cytometry.

Figure S5

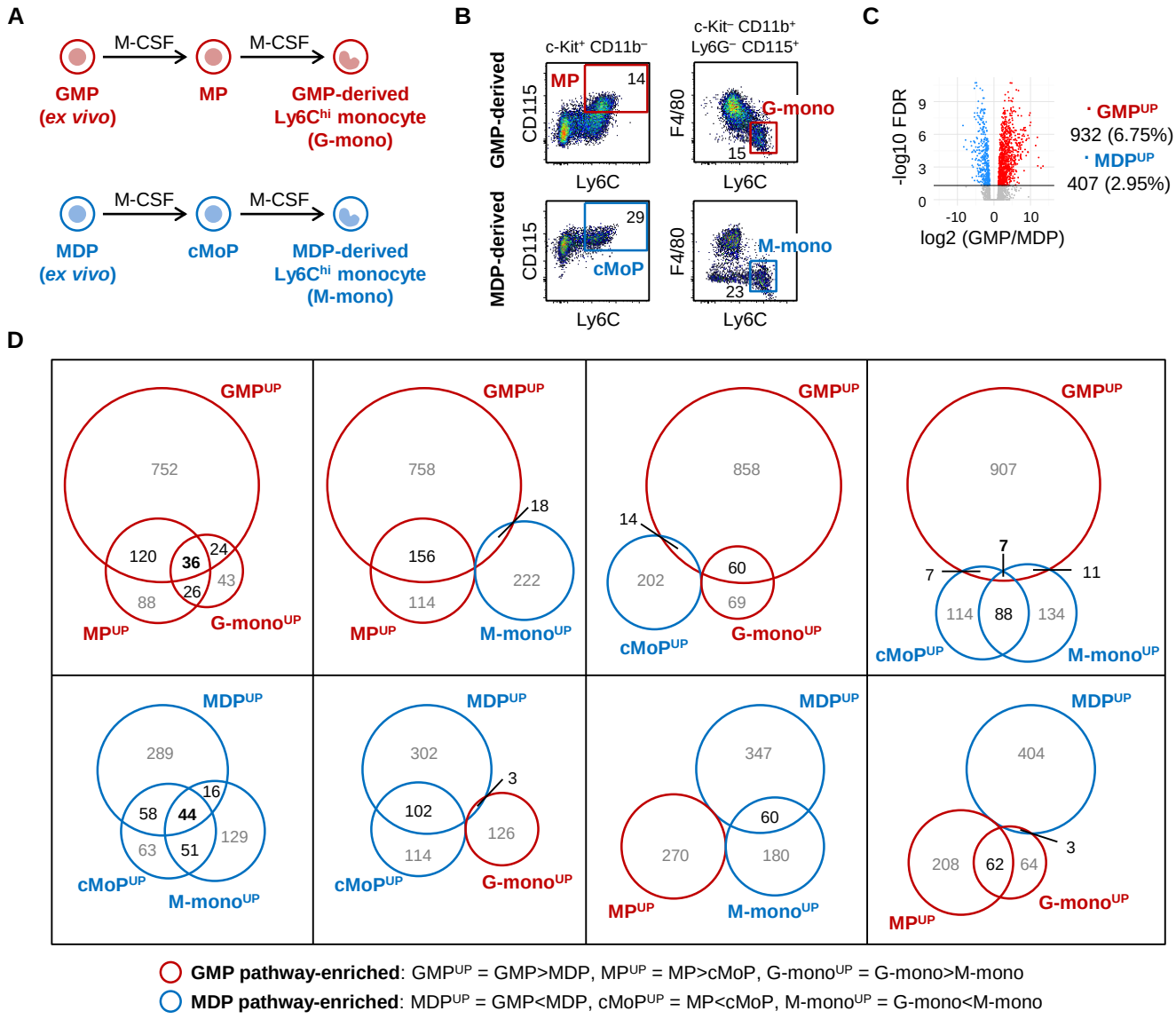

Figure S5. Isolation of GMP- and MDP-derived cells for RNA sequencing. (related to Figure 3)

(A-B) GMPs and MDPs isolated from the pooled bone marrow of 20 mice were cultured *in vitro* with M-CSF to derive monocyte-committed progenitors (MPs and cMoPs) and Ly6C^{hi} monocytes. Monocyte progenitors and Ly6C^{hi} monocytes derived from GMPs (MPs and G-mono) and MDPs (cMoPs and M-mono) were harvested from the cultures on days 2, 3 and 4, and the three timepoint samples were pooled for RNA extraction. RNA was also extracted from the *ex vivo* GMP and MDP fractions from which the monocyte progenitors and monocytes were derived. The whole process was repeated using 20 additional mice to obtain a replicate set of samples. (C) Volcano plot of genes enriched (2-fold, adjusted p value < 0.05) in GMPs (GMP^{UP}) versus MDPs (MDP^{UP}). The number of enriched genes and percentage of the total genes expressed by GMPs and MDP is indicated. (D) Venn diagrams (plotted to scale) showing overlapping sets of enriched genes (^{UP} = enriched in the specified subset compared to its counterpart in the other lineage).

Figure S6

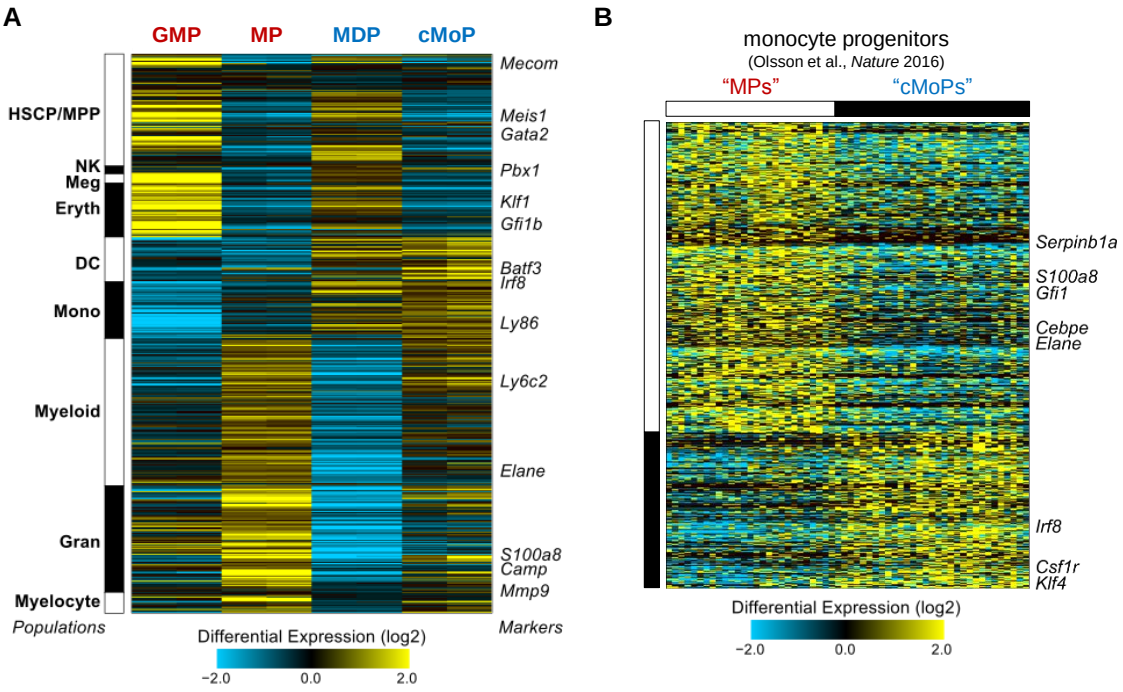

Figure S6. Profiling of GMP- and MDP-derived monocyte progenitor subsets. (related to Figure 3) (A) Gene expression by the progenitors (GMPs, MPs, MDPs and cMoPs) was viewed through the lens of progenitor population-specific genes and selected markers previously defined in a single-cell RNA sequencing study (Olsson et al., 2016). All genes with an RPKM>1 are shown. HSCP/MPP – hematopoietic stem cell progenitor, NK – natural killer cell, Meg – megakaryocyte, Eryth – erythrocyte, DC – dendritic cell, Mono – monocyte, Gran – granulocyte, Myelocyte – myelocyte and metamyelocyte. (B) Heatmap of differential gene expression (2-fold, $p<0.05$) by the presumed MPs and cMoPs ("MPs" and "cMoPs") among the 58 previously identified monocyte progenitors profiled by single-cell RNA sequencing (Olsson et al., 2016).

Figure S7

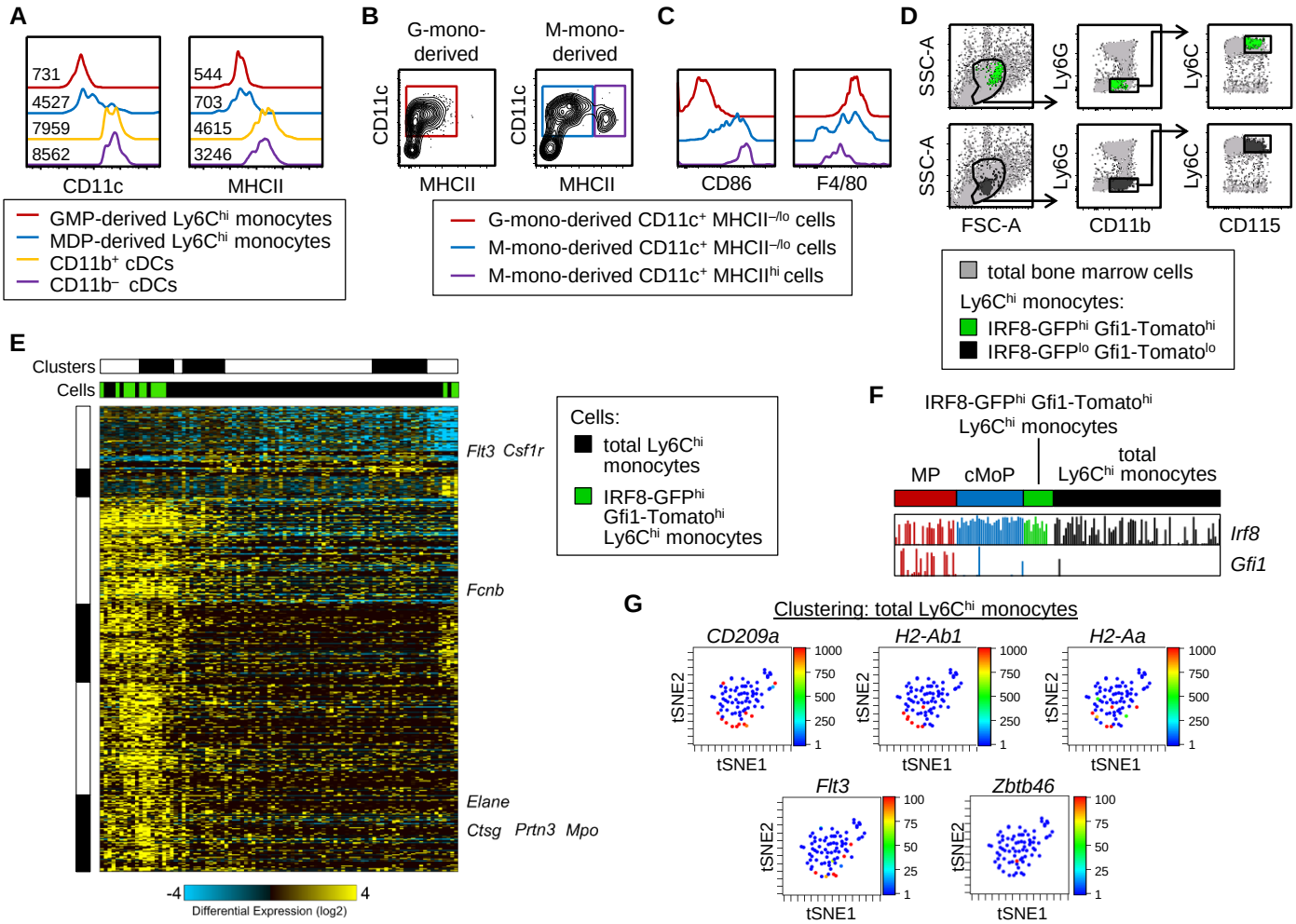

Figure S7. Single-cell RNA sequencing of Ly6C^{hi} monocytes. (related to Figures 4-6)

(A) CD11c (surface) and MHCII (surface and intracellular) expression by splenic Ly6C^{hi} monocytes derived from adoptively transferred GMPs and MDPs, as well as endogenous DCs, was assessed by flow cytometry. MFI values are indicated. (B-C) Ly6C^{hi} monocytes were sorted from 3-day *in vitro* cultures of GMPs and MDPs with M-CSF, and then cultured with GM-CSF for a further 4 days prior to assessment of CD11c and MHCII expression by flow cytometry (B). CD86 and F4/80 expression by subsets of CD11c^{+} cells was also assessed by flow cytometry (C). (D) Back-gating of Ly6C^{hi} monocyte subsets from IRF8-GFP Gfi1-tdTomato reporter mouse bone marrow. (E-G) Gene expression by Ly6C^{hi} monocytes from the bone marrow of wild-type and IRF8-GFP Gfi1-tdTomato reporter mice (78 and 14 monocytes, respectively) was assessed by single-cell RNA sequencing. (E) Unsupervised clustering of Ly6C^{hi} monocytes using ICGS in AltAnalyze. (F) Comb plots of transcription factor expression by individual Ly6C^{hi} monocytes and monocyte progenitors. (G) Total wild-type Ly6C^{hi} monocytes were also clustered using Cytobank (tSNE plots are shown). Clustering was performed using 252 genes that were differentially expressed in GMP- and MDP-derived Ly6C^{hi} monocytes (G-mono^{UP} and M-mono^{UP} genes identified by bulk sequencing) and also detected by single-cell RNA sequencing. Expression intensities (log10 RPKM) of moDC-producing monocyte markers (*CD209a*, *H2-Ab1*, *H2-Aa* and *Flt3*) and the cDC transcription factor *Zbtb46* are shown.